

Boundary and Interface Conditions for High-Order Finite-Difference Methods Applied to the Euler and Navier–Stokes Equations

Jan Nordström* and Mark H. Carpenter†

**FFA, The Aeronautical Research Institute of Sweden, Bromma, Sweden and the Department of Scientific Computing, Uppsala University, Uppsala, Sweden;*

†*Aerodynamic and Acoustic Methods Branch,
NASA Langley Research Center, Hampton, VA 23681*

E-mail: nmj@ffa.se

Received April 6, 1998; revised October 15, 1998

Boundary and interface conditions for high-order finite difference methods applied to the constant coefficient Euler and Navier–Stokes equations are derived. The boundary conditions lead to strict and strong stability. The interface conditions are stable and conservative even if the finite difference operators and mesh sizes vary from domain to domain. Numerical experiments show that the new conditions also lead to good results for the corresponding nonlinear problems. © 1999 Academic Press

1. INTRODUCTION

In many computational problems, low-order finite difference methods (second order or less) are not accurate enough. Examples in which high-frequency components in the solution must be resolved by using high-order finite difference methods (HOFDM) include aeroacoustics, turbulence, and transition simulations, the propagation and scattering of electromagnetic waves, and simulation of reactive flows at high speeds [1, 6]. The efficiency [7] of HOFDM can be used either to increase the accuracy for a fixed number of mesh points *or* to reduce the computational cost for a given accuracy by reducing the number of mesh points.

The main reason that low-order finite difference methods are used in practical calculations is because of the difficulty that arises for HOFDM near the boundaries of the computational domain. On a Cartesian mesh, it is quite easy to derive nonsymmetric boundary operators that have high formal accuracy; the difficulty is to derive highly accurate *and* stable operators. In [8, 9] HOFDM are constructed based on the work in [10, 11]. In these strictly stable schemes, the growth rates of the analytic and semidiscrete solution are identical. Strict stability is

obtained by constructing discrete operators that satisfy a summation-by-parts (SBP) rule which mimics the integration-by-parts rule in the continuous case. For calculations over long times, strict stability is very important because it prevents error growth in time for fixed Δx .

In [12] it was shown that many G-K-S stable [13] (convergence to true true solution as $\Delta x \rightarrow 0$) scalar schemes were not strictly stable. Moreover, many scalar schemes that were both G-K-S stable and strictly stable exhibit time growth when they are applied to systems of equations. The underlying reason for the error growth in time is caused by the way the mathematical boundary conditions were imposed. An orthogonal projection operator is used to impose the mathematical boundary conditions in [14, 15]. In the so-called SAT (simultaneous approximation term) procedure [16], a linear combination of the boundary conditions in the form of a forcing function and the differential equations is solved near the boundary. Both these methods impose the correct boundary conditions and preserve strict stability.

Another important concept is strong stability. An approximation is strongly stable if the solution, including the values at the boundary points, can be estimated in terms of all data in the problem [17]. The stability estimate in the strongly stable case leads directly to the error estimate if no extra or numerical boundary conditions are necessary. Stability analysis using the Laplace transform technique leads to strong stability if the Kreiss condition is satisfied; see [18, 9, paper IV]. Note that strict stability leads to strong stability, but strong stability does not imply strict stability.

Most investigations regarding HOFDM are done on linear hyperbolic model equations with constant coefficients on a uniform mesh. However, nonlinear Navier–Stokes calculations on nonuniform meshes have been performed [19]. One of the conclusions in [19] was that the treatment of the metric derivatives is a crucial point for nonsmooth meshes. This problem is analyzed in [20], where so-called mimetic difference operators (discrete operators with the same symmetry properties as the continuous operators) are derived. In [15], strict stability for parabolic and hyperbolic systems in curvilinear coordinates on a single domain were investigated.

Generating a smooth grid around a complex configuration can be very difficult, if not impossible, and is often the most time-consuming aspect of the solution procedure. This fact has limited the use of HOFDM in practical calculations to the small class of simple geometries which can be smoothly mapped onto the unit cube. In this paper we consider a structured multiblock approach in which each subdomain is discretized by using a discrete operator with the SBP property. The subdomains are patched together to a global domain by using suitable interface conditions. This technique was used in [21–23] for Chebyshev spectral methods.

In [24], stable and conservative interface conditions for HOFDM applied to the scalar advection–diffusion equation on multiple domains were derived. In each subdomain the step size was constant but significantly different from that in the adjacent subdomains. Also, the finite difference operators could vary from subdomain to subdomain. In this paper we will generalize the results in [24] and extend the analysis to the one-dimensional constant coefficient Euler and Navier–Stokes equations.

The rest of this paper will proceed as follows. In Section 2, some basic definitions are given. In Section 3, the Navier–Stokes equations in conservative, primitive, and characteristic variable form are given. In Section 4, the continuous problem is analyzed, while the discrete problem is investigated in Section 5. Numerical experiments are performed in Section 6 and we summarize and draw conclusions in Section 7.

2. DEFINITIONS

Consider the linear initial boundary value problem

$$\begin{aligned} w_t &= Pw + \delta F(x, t), & x \in \Omega; t \geq 0, \\ w &= \delta f(x), & x \in \Omega; t = 0, \\ L_C w &= \delta g(t), & x \in \Gamma; t \geq 0, \end{aligned} \tag{1}$$

where P is the differential operator and L_C is the boundary operator. The initial function δf , the forcing function δF , and the boundary data δg are the data of the problem; w denotes the difference between a solution with data f, F, g and one with data $f + \delta f, F + \delta F, g + \delta g$.

There are many concepts of well posedness (see [17]). Here we consider the following definition.

DEFINITION 1. The problem (1) is strongly well posed if the solution w is unique, exists, and satisfies

$$\|w\|_{\Omega}^2 + \int_0^t \|w\|_{\Gamma}^2 dt \leq K_c e^{\eta_c t} \left\{ \|\delta f\|_{\Omega}^2 + \int_0^t (\|\delta F\|_{\Omega}^2 + \|\delta g\|_{\Gamma}^2) dt \right\}, \tag{2}$$

where K_c and η_c may not depend on $\delta F, \delta f, \delta g$. $\|\cdot\|_{\Omega}$ and $\|\cdot\|_{\Gamma}$ are suitable continuous norms.

The semidiscrete version of (1) is

$$\begin{aligned} (w_j)_t &= Qw_j + \delta F_j(t), & x_j \in \Omega; t \geq 0, \\ w_j &= \delta f_j, & x_j \in \Omega; t = 0, \\ L_D w_j &= \delta g(t), & x_j \in \Gamma; t \geq 0, \end{aligned} \tag{3}$$

where Q is the difference operator approximating the differential operator P , δF_j is the forcing function, δf_j is the initial function, L_D is the discrete boundary operator, where numerical boundary conditions are included, and δg is the boundary data. It is assumed that (3) is a consistent approximation of (1).

Closely related to the concept of well posedness is the concept of stability.

DEFINITION 2. The problem (3) is strongly stable, if for a sufficiently fine mesh, the solution w_j satisfies

$$\|w\|_{\Omega}^2 + \int_0^t \|w\|_{\Gamma}^2 dt \leq K_d e^{\eta_d t} \left\{ \|\delta f\|_{\Omega}^2 + \int_0^t (\|\delta F\|_{\Omega}^2 + \|\delta g\|_{\Gamma}^2) dt \right\}, \tag{4}$$

where K_d and η_d may not depend on $\delta F_j, \delta f_j, \delta g$. $\|\cdot\|_{\Omega}$ and $\|\cdot\|_{\Gamma}$ are suitable discrete norms.

DEFINITION 3. The approximation (3) of (1) is strictly stable if the analytical and discrete growth rates (see (2) and (4)) satisfy

$$\eta_d \leq \eta_c + \mathcal{O}(\Delta x), \tag{5}$$

where Δx is the mesh size.

For later reference we also define some useful matrix operations; see [25].

DEFINITION 4. Let A be a $p \times q$ matrix and let B be an $m \times n$ matrix, then

$$A \otimes B = \begin{pmatrix} a_{0,0}B & \cdots & a_{0,q-1}B \\ \vdots & & \vdots \\ a_{p-1,0}B & \cdots & a_{p-1,q-1}B \end{pmatrix}.$$

The $p \times q$ block matrix $A \otimes B$ is called a Kronecker product.

There are a number of rules for Kronecker products (see [25]). In this paper we will make use of

$$(A \otimes B)(C \otimes D) = (AC) \otimes (BD), \quad (A \otimes B)^T = A^T \otimes B^T. \quad (6)$$

The following lemma will be used frequently below; it is a direct consequence of the first rule in (6).

LEMMA 1. Let A be an $m \times m$ matrix, let B be an $n \times n$ matrix, let $\tilde{A} = I_n \otimes A$, and let $\tilde{B} = B \otimes I_m$; then $\tilde{A}\tilde{B} = \tilde{B}\tilde{A}$.

3. THE EULER AND NAVIER-STOKES EQUATIONS

The one-dimensional constant coefficient Navier-Stokes equations in primitive (W), characteristic (C), and conservative (Q) variable form are

$$W_t + \bar{A}W_x = \epsilon \bar{B}W_{xx}, \quad C_t + \bar{\Lambda}C_x = \epsilon \bar{X}C_{xx}, \quad Q_t + F_x^I = \epsilon F_x^V, \quad (7)$$

respectively. With $\epsilon = 0$, Eq. (7) becomes the one-dimensional constant coefficient Euler equations. The overbar is used to denote variables with a constant state. The relation between W , C , Q , where $W = (\rho, u, T)^T$ is

$$C = \bar{R}\bar{S}W, \quad Q = \bar{T}W, \quad (8)$$

where

$$\bar{R} = \begin{pmatrix} -1/\sqrt{2\gamma} & 1/\sqrt{2} & -\sqrt{(\gamma-1)/2\gamma} \\ \sqrt{(\gamma-1)/\gamma} & 0 & -1/\sqrt{\gamma} \\ 1/\sqrt{2\gamma} & 1/\sqrt{2} & \sqrt{(\gamma-1)/2\gamma} \end{pmatrix},$$

$$\bar{S} = \sqrt{2} \begin{pmatrix} \bar{c}^2/\sqrt{\gamma} & 0 & 0 \\ 0 & \bar{\rho}\bar{c} & 0 \\ 0 & 0 & \bar{\rho}/\sqrt{\gamma(\gamma-1)M_\infty^4} \end{pmatrix},$$

$$\bar{T} = \begin{pmatrix} 1 & 0 & 0 \\ \bar{u} & \bar{\rho} & 0 \\ \bar{c}^2/(\gamma(\gamma-1)) + \bar{u}^2/2 & \bar{\rho}\bar{u} & \bar{\rho}/(\gamma(\gamma-1)M_\infty^2) \end{pmatrix}.$$

Note that $\bar{R}\bar{R}^T = I_3$.

The transformation (8) implies that the matrices and fluxes in (7) are

$$\bar{A} = \begin{pmatrix} \bar{u} & \bar{\rho} & 0 \\ \bar{c}^2/\gamma\bar{\rho} & \bar{u} & 1/\gamma M_\infty^2 \\ 0 & (\gamma - 1)\bar{c}^2 M_\infty^2 & \bar{u} \end{pmatrix}, \tag{9}$$

$$\bar{B} = \begin{pmatrix} 0 & 0 & 0 \\ 0 & (\bar{\lambda} + 2\bar{\mu})/\bar{\rho} & 0 \\ 0 & 0 & \gamma\bar{\kappa}/(Pr\bar{\rho}) \end{pmatrix}, \tag{10}$$

$$\bar{\Lambda} = \begin{pmatrix} \bar{u} - \bar{c} & 0 & 0 \\ 0 & \bar{u} & 0 \\ 0 & & \bar{u} + \bar{c} \end{pmatrix}, \quad \bar{X} = \frac{1}{2} \begin{pmatrix} \bar{\theta} + \bar{\phi} & \alpha\bar{\phi} & \bar{\theta} - \bar{\phi} \\ \alpha\bar{\phi} & \alpha^2\bar{\phi} & -\alpha\bar{\phi} \\ \bar{\theta} - \bar{\phi} & -\alpha\bar{\phi} & \bar{\theta} + \bar{\phi} \end{pmatrix}, \tag{11}$$

$$F^I = \bar{T}\bar{A}W = \bar{T}\bar{A}\bar{T}^{-1}Q, \quad F^V = \bar{T}\bar{B}W_x = \bar{T}\bar{B}\bar{T}^{-1}Q_x. \tag{12}$$

The dependent variables and parameters $\rho, u, T, p, c, M_\infty, \mu, \lambda, \kappa, Pr, \gamma,$ and ϵ are respectively the density, x, y, z components of the velocity, the temperature, the pressure, the speed of sound, the free-stream Mach number, the shear, and second viscosity, the coefficient of heat conduction, the Prandtl number, the ratio of specific heats, and the inverse Reynolds number. The notations $\bar{\theta} = (\bar{\lambda} + 2\bar{\mu})/\bar{\rho}, \bar{\phi} = (\gamma - 1)\bar{\kappa}/(Pr\bar{\rho}), \alpha = \sqrt{2/(\gamma - 1)}$ have also been introduced.

4. THE CONTINUOUS PROBLEM

In this paper we will consider interface conditions between subdomains. However, interface conditions are closely related to boundary conditions; therefore, we start with the single domain problem.

4.1. The Continuous Single Domain Problem

To make the presentation self-contained, some results in [27] are included in this section. Consider the Navier–Stokes equations on characteristic form,

$$\begin{aligned} C_t + \bar{\Lambda}C_x &= \epsilon\bar{X}C_{xx} + F(x, t), & t \geq 0; -1 \leq x \leq 1, \\ C &= f(x), & t = 0; -1 \leq x \leq 1, \\ L_{-1}C &= g_{-1}(t), & t \geq 0; x = -1, \\ L_{+1}C &= g_{+1}(t), & t \geq 0; x = +1, \end{aligned} \tag{13}$$

where $C = (\bar{\rho}\bar{c}u - p, \alpha(\bar{\rho}\bar{c}^2 - p), \bar{\rho}\bar{c}u + p)^T, 0 < \epsilon \ll 1,$ and L_{-1}, L_{+1} are the boundary operators. For $\bar{u} > 0,$ there is inflow at $x = -1$ and outflow at $x = 1.$

4.1.1. Well Posedness

Let

$$(U, V) = \int_{-1}^{+1} U^T V dx, \quad (U, U) = \|U\|^2, \quad \|U\|_1^2 = |U|_{x=-1}^2 + |U|_{x=+1}^2$$

denote the L_2 scalar product, the L_2 norm, and the boundary norm, respectively. The boundary conditions (see [27, 22]),

$$L_{-1}C = \frac{(\bar{\Lambda} + |\bar{\Lambda}|)}{2}C - \epsilon \bar{X}C_x = g_{-1}, \quad (14)$$

$$L_{+1}C = \left\{ \frac{(\bar{\Lambda} - |\bar{\Lambda}|)}{2}C - \epsilon \bar{X}C_x \right\}_i = \{g_{+1}\}_i, \quad i = 1, 2, \quad (15)$$

and the energy method applied to (13) leads to

$$\begin{aligned} \|C\|_t^2 = & -2\epsilon(C_x, \bar{X}C_x) + 2(C, F) - [C^T \Lambda_I C - 2C^T g_{-1}]_{x=-1} \\ & - [C^T \Lambda_O C + 2C^T g_{+1}]_{x=+1}. \end{aligned} \quad (16)$$

In (14)–(16), $g_{+1} = (g_1, g_2, g_1 - (2/\alpha)g_2)^T$, $|\bar{\Lambda}| = \text{diag}(|\lambda_1|, |\lambda_2|, |\lambda_3|)$, and

$$\Lambda_I = |\bar{\Lambda}|, \quad \Lambda_O = \begin{pmatrix} |\lambda_1| & 0 & (|\lambda_1| - \lambda_1)/2 \\ 0 & |\lambda_2| & 0 \\ (|\lambda_1| - \lambda_1)/2 & 0 & |\lambda_3| \end{pmatrix}. \quad (17)$$

Integration of (16) leads to

$$\begin{aligned} \|C\|^2 + e^{\eta T} \left\{ 2\epsilon \int_0^T (C_x, \bar{X}C_x) e^{-\eta t} dt + \frac{\delta}{2} \int_0^T \|C\|_t^2 e^{-\eta t} dt \right\} \\ \leq e^{\eta T} \left\{ \|f\|^2 + \frac{2}{\delta} \int_0^T \|g\|_t^2 e^{-\eta t} dt + \frac{1}{\eta} \int_0^T \|F\|^2 e^{-\eta t} dt \right\}, \end{aligned} \quad (18)$$

where $0 < \eta < 1$, $\delta = \min|d_j|$, $D = |\bar{\Lambda}|H$, and

$$H = \text{diag}(H_1, 1, H_3), \quad H_1 = \frac{|\lambda_3| - |\lambda_1|}{|\lambda_3| + |\lambda_3|}, \quad H_3 = \frac{|\lambda_3| - |\lambda_1|}{|\lambda_3| + |\lambda_3|}.$$

Note that (14), (15) reduce to the characteristic boundary conditions for the Euler equations as $\epsilon \rightarrow 0$.

Uniqueness follows directly from the estimate (18). Existence can be shown by using the Laplace-transform technique or via difference approximations; see [26, 28]. Since (18) is of the form (2), we can conclude that the following theorem holds.

THEOREM 1. *The problem (13), (14), (15) is strongly well posed.*

4.2. The Continuous Multiple Domain Problem

In this section we split the domain $[-1, 1]$ into $[-1, 0]$ and $[0, 1]$ and focus on the interface problem at $x = 0$. The two coupled problems are

$$\begin{aligned} U_t + \bar{\Lambda}U_x &= \epsilon \bar{X}U_{xx} + F(x, t), & t \geq 0; \quad -1 \leq x \leq 0, \\ U &= f(x), & t = 0; \quad -1 \leq x \leq 0, \\ L_{-1}U &= g_{-1}(t), & t \geq 0; \quad x = -1, \\ L_0(U - V) &= 0, & t \geq 0; \quad x = 0; \end{aligned} \quad (19)$$

$$\begin{aligned}
 V_t + \bar{\Lambda} V_x &= \epsilon \bar{X} V_{xx} + F(x, t), & t \geq 0; 0 \leq x \leq +1, \\
 V &= f(x), & t = 0; 0 \leq x \leq +1, \\
 L_0(V - U) &= 0, & t \geq 0; x = 0, \\
 L_{+1} V &= g_{+1}(t), & t \geq 0; x = +1,
 \end{aligned} \tag{20}$$

respectively. The characteristic variables in the left $[-1, 0]$ and right $[0, +1]$ domain are U and V , respectively. The coupling between (19) and (20) is given by the operator L_0 .

By subtracting (13) from (19)–(20), by transforming the problem on $[0, +1]$ onto $[-1, 0]$ via the transformation $x \rightarrow -\xi$, and finally by replacing ξ with x , we obtain

$$\begin{aligned}
 \psi_t + \tilde{\Lambda} \psi_x &= \epsilon \tilde{X} \psi_{xx}, & t \geq 0; -1 \leq x \leq 0, \\
 \psi &= 0, & t = 0; -1 \leq x \leq 0, \\
 L_{-1} \tilde{U} &= 0, & t \geq 0; x = -1, \\
 \tilde{L}_{+1} \tilde{V} &= 0, & t \geq 0; x = -1, \\
 \tilde{L}_0(\tilde{U} - \tilde{V}) &= 0, & t \geq 0; x = 0,
 \end{aligned} \tag{21}$$

where

$$\psi = \begin{pmatrix} \tilde{U} \\ \tilde{V} \end{pmatrix} = \begin{pmatrix} U - C \\ V - C \end{pmatrix}, \quad \tilde{\Lambda} = \begin{pmatrix} +\bar{\Lambda} & 0 \\ 0 & -\bar{\Lambda} \end{pmatrix}, \quad \tilde{X} = \begin{pmatrix} \bar{X} & 0 \\ 0 & \bar{X} \end{pmatrix},$$

and

$$L_{-1} \tilde{U} = \frac{(\bar{\Lambda} + |\bar{\Lambda}|)}{2} \tilde{U} - \epsilon \tilde{X} \tilde{U}_x, \quad \tilde{L}_{+1} \tilde{V} = \left\{ \frac{(\bar{\Lambda} - |\bar{\Lambda}|)}{2} \tilde{V} + \epsilon \tilde{X} \tilde{V}_x \right\}_i, \quad i = 1, 2. \tag{22}$$

4.2.1. Well Posedness

The energy method applied to (21) leads to

$$\|\psi\|_t^2 = [\psi^T \tilde{\Lambda} \psi - 2\epsilon \psi^T \tilde{X} \psi_x]_{x=0}^{x=-1} - 2\epsilon(\psi_x, \tilde{X} \psi_x).$$

The analysis of the single domain problem implies that the boundary terms at $x = -1$ are negative semidefinite with the boundary operators (22). At the interface $x = 0$, we have

$$\begin{aligned}
 & [\psi^T \tilde{\Lambda} \psi - 2\epsilon \psi^T \tilde{X} \psi_x]_{x=0} \\
 &= \frac{1}{2} \begin{pmatrix} \tilde{U} - \tilde{V} \\ \tilde{U} + \tilde{V} \\ (\tilde{U} - \tilde{V})_x \\ (\tilde{U} + \tilde{V})_x \end{pmatrix} \begin{pmatrix} 0 & \bar{\Lambda} & -\epsilon \bar{X} & 0 \\ \bar{\Lambda} & 0 & 0 & -\epsilon \bar{X} \\ -\epsilon \bar{X} & 0 & 0 & 0 \\ 0 & -\epsilon \bar{X} & 0 & 0 \end{pmatrix} \begin{pmatrix} \tilde{U} - \tilde{V} \\ \tilde{U} + \tilde{V} \\ (\tilde{U} - \tilde{V})_x \\ (\tilde{U} + \tilde{V})_x \end{pmatrix}. \tag{23}
 \end{aligned}$$

Well posedness for the Euler equations ($\epsilon = 0$) requires $\tilde{U} - \tilde{V} = 0$ since $\bar{\Lambda}$ is nonsingular. With that choice we get

$$[\psi^T \tilde{\Lambda} \psi - 2\epsilon \psi^T \tilde{X} \psi_x]_{x=0} = -2\epsilon \tilde{U}^T \tilde{X} (\tilde{U} + \tilde{V})_x = -2\epsilon ((\bar{R}\bar{S})^T \tilde{U})^T \bar{B} (W_1 + W_2)_x,$$

where $(\bar{R}\bar{S})^{-1}U = W_L$, $(\bar{R}\bar{S})^{-1}V = W_R$ denotes the primitive variables in the left and right domain, respectively. The structure of \bar{B} (see (10)) and a transformation to the original coordinate system lead to the following theorem.

THEOREM 2. *If theorem 1 holds and the interface conditions*

$$\begin{pmatrix} I_3 \\ \epsilon D_1 \end{pmatrix} \begin{pmatrix} U - V \\ (U - V)_x \end{pmatrix} = 0, \quad D_1 = \begin{pmatrix} 1 & 0 & 1 \\ 1 & \alpha & -1 \end{pmatrix} \quad (24)$$

are used, then (19) and (20) are strongly well posed.

Remark. The problems (19) and (20) are strongly well posed in the sense that the solutions can be estimated in terms of the data in the corresponding one domain problem (13).

Remark. The condition (24) in primitive variable formulation is

$$\begin{pmatrix} I_3 \\ \epsilon D_2 \end{pmatrix} \begin{pmatrix} W_L - W_R \\ (W_L - W_R)_x \end{pmatrix} = 0, \quad D_2 = \begin{pmatrix} 0 & 1 & 0 \\ 0 & 0 & 1 \end{pmatrix}.$$

5. THE DISCRETE PROBLEM

Let $U, \mathcal{D}U$ be the numerical approximations of the scalar quantities u and u_x , respectively. The approximation $\mathcal{D}U$ of the first derivative

$$\mathcal{D}U = P^{-1}QU, \quad Pu_x - Qu = PT_{e1}, \quad |T_{e1}| = \mathcal{O}(\Delta x^m, \Delta x^n)$$

satisfies the SBP rule,

$$(U, DV)_P = U_N V_N - U_0 V_0 - (\mathcal{D}U, V)_P, \quad (25)$$

where

$$(U, V)_P = U^T P V, \quad P = P^T, \quad Q + Q^T = D, \quad D = \text{diag}[-1, 0, \dots, 0, 1] \quad (26)$$

and $0 < p_{\min} \Delta x I \leq P \leq p_{\max} \Delta x I$. Operators of the SBP type arise naturally with centered difference approximations, for example, see [11, 29, 12, 30].

The second derivative can be obtained by applying the first derivative operator twice. Such an approximation satisfies the SBP rule (25) exactly. However, there are drawbacks with such a procedure. A second derivative formed in that way is unnecessarily wide and inaccurate and can lead to odd-even mode decoupling. A second derivative operator with the properties

$$\mathcal{D}^2 U = P^{-1} R U, \quad Pu_{xx} - Ru = PT_{e2}, \quad T_{e2} = \mathcal{O}(\Delta x^m, \Delta x^n), \quad (27)$$

$$R = (-S^T M + D) S, \quad (28)$$

was suggested in [24]. The matrix D is given in (26); M is positive definite, i.e., $U^T M U > 0$ and $0 < m_{\min} \Delta x I \leq M \leq m_{\max} \Delta x I$.

S is a diagonal matrix with a discrete representation of the first derivative on the first and last rows,

$$\{Su\}_0 = \{\mathcal{D}u\}_0 = u_x(x_0, t) + T_{e3}, \quad \{Su\}_n = \{\mathcal{D}u\}_n = u_x(x_n, t) + T_{e3},$$

where $|T_{e3}| = \mathcal{O}(\Delta x^r)$ and

$$S = \frac{1}{\Delta x} \begin{pmatrix} s_{00} & s_{01} & s_{02} & s_{03} & \cdots & & & & & & \\ 0 & 1 & 0 & & & & & & & & & \\ & & 0 & 1 & 0 & & & & & & & \\ & & & \ddots & \ddots & \ddots & & & & & & \\ & & & & 0 & 1 & 0 & & & & & \\ & & & & & 0 & 1 & 0 & & & & \\ \cdots & & & \cdots & s_{nn-3} & s_{nn-2} & s_{nn-1} & s_{nn} & & & & \end{pmatrix}.$$

The second derivative defined in (27) and (28) satisfies a modified SBP rule. We have

$$(U, \mathcal{D}^2 V)_P = U_n \{\mathcal{D}V\}_n - U_0 \{\mathcal{D}V\}_0 - (SU)^T M (SV).$$

The notation $|T_{e1}|, |T_{e2}| = \mathcal{O}(\Delta x^m, \Delta x^n)$ and $|T_{e3}| = \mathcal{O}(\Delta x^r)$ means that the approximation of the differential operator is accurate to order m in the interior of the domain, to order n at the boundary, and that the approximation of the boundary conditions is accurate to order r . The relation between the different orders of accuracy, i.e., m, n, r , is discussed in Section 5.1.2 below.

So far we have considered difference approximations of scalar quantities. The corresponding approximations for vector quantities are defined by using Kronecker products (see Definition 4). The spatial operators $\mathcal{D}, \mathcal{D}^2$ and the matrices that define them are of the form $B \otimes I_3$ in this paper. As an example, $P^{-1}Q$ means $(P^{-1} \otimes I_3)(Q \otimes I_3) = P^{-1}Q \otimes I_3$. In the sequel, that notation is implied.

Let $H = H^T > 0$; for later reference we introduce the notations

$$(U, V)_H = U^T H V, \quad (U, U)_H = \|U\|_H^2, \quad \|U\|_{\Gamma_D}^2 = |U|_{i=0}^2 + |U|_{i=n}^2. \tag{29}$$

5.1. The Discrete Single Domain Problem

We introduce a uniform mesh $x_i = -1 + i \Delta x, x_0 = -1, x_n = +1$. The finite difference approximation of (13) with the SAT technique [16] for boundary conditions is

$$\begin{aligned} C_t + \tilde{\Lambda} D C &= \epsilon \tilde{X} \mathcal{D}^2 C + F + P^{-1} [\sigma_{-1} (L_{-1}^D C - g_{-1}) e_{-1} + \sigma_{+1} (L_{+1}^D C - g_{+1}) e_{+1}], \\ C(0) &= f, \end{aligned} \tag{30}$$

where

$$D = P^{-1} Q \otimes I_3, \quad \mathcal{D}^2 = P^{-1} R \otimes I_3, \tag{31}$$

$$R = Q P^{-1} Q \otimes I_3, \quad \text{or} \quad R = (-S^T M + D) S \otimes I_3, \tag{32}$$

$$\tilde{\Lambda} = I_n \otimes \bar{\Lambda}, \quad \tilde{X} = I_n \otimes \bar{X}, \quad e_{-1} = (1, \dots, 0)^T \otimes I_3, \quad e_{+1} = (0, \dots, 1)^T \otimes I_3. \tag{33}$$

The unknown diagonal matrices σ_{-1} and σ_{+1} will be determined below.

5.1.1. *Stability*

The energy method leads to

$$\begin{aligned} \frac{d}{dt} \|C\|_P^2 &= -C^T(\tilde{\Lambda}Q + Q^T\tilde{\Lambda})C + \epsilon C^T(\tilde{X}R + R^T\tilde{X})C + 2(C, F)_P \\ &\quad + 2C_0^T\sigma_{-1}[L_{-1}^D C - g_{-1}] + 2C_N^T\sigma_{+1}[L_{+1}^D C - g_{+1}]. \end{aligned} \quad (34)$$

The definition of the first derivative operator $P^{-1}Q$ and Lemma 1 leads to

$$-C^T(\tilde{\Lambda}Q + Q^T\tilde{\Lambda})C = C_0^T\bar{\Lambda}C_0 - C_n^T\bar{\Lambda}C_n. \quad (35)$$

The definition of the second derivative operators $R = (-S^T M + D)S$ and $R = QP^{-1}Q$ yields

$$C^T(\tilde{X}R + R^T\tilde{X})C = -2C_0\bar{X}DC_0 + 2C_n\bar{X}DC_n - (SC)^T(\tilde{X}M + (\tilde{X}M)^T)(SC) \quad (36)$$

$$C^T(\tilde{X}R + R^T\tilde{X})C = -2C_0\bar{X}DC_0 + 2C_n\bar{X}DC_n - 2(P^{-1}QC)^T P\tilde{X}P^{-1}QC, \quad (37)$$

respectively.

By introducing (35), (36), and (37) into (34) we get

$$\begin{aligned} \frac{d}{dt} \|C\|_P^2 + 2\epsilon(DC, \tilde{X}DC)_H &= [C^T\bar{\Lambda}C - 2\epsilon C^T\bar{X}DC]_{i=n}^{i=0} + 2(C, F)_P \\ &\quad + 2C_0^T\sigma_{-1}[L_{-1}^D C - g_{-1}] + 2C_N^T\sigma_{+1}[L_{+1}^D C - g_{+1}], \end{aligned} \quad (38)$$

where the scalar products and norms are defined in (29).

The boundary operators L_{-1}^D, L_{+1}^D are the discrete versions of (14)–(15), with one important modification. In [27] it is shown that the two outflow conditions in (15) determine the value of the last row of $\bar{X}C_x$ in terms of the in-going characteristic variable and boundary data; i.e., (15) implies that

$$\{-\epsilon\bar{X}C_x\}_3 = -\frac{\lambda_1 - |\lambda_1|}{2}C_1 + g_1 - (2/\alpha)g_2, \quad x = +1. \quad (39)$$

To explicitly incorporate (39) into (30) we use

$$L_{-1}^D C = \left\{ \frac{(\bar{\Lambda} + |\bar{\Lambda}|)}{2} C - \epsilon\bar{X}DC \right\}_{i=0} = g_{-1}, \quad (40)$$

$$L_{+1}^D C = \left\{ \frac{(\bar{\Lambda} - |\bar{\Lambda}|)}{2} C - \epsilon\bar{X}DC \right\}_{i=n} = g_{+1}, \quad (41)$$

where $(g_{+1})_3$ is equal to the right-hand side of (39). The boundary conditions (40), (41) inserted in (38) yield

$$\begin{aligned} \frac{d}{dt} \|C\|_P^2 &= -2\epsilon(DC, \tilde{X}DC)_H + 2(C, F)_P + \{C^T[\bar{\Lambda} + \sigma_{-1}(\bar{\Lambda} + |\bar{\Lambda}|)]C\}_{i=0} \\ &\quad + \{C^T[-2\epsilon\bar{X} - 2\epsilon\sigma_{-1}\bar{X}]DC\}_{i=0} + \{C^T[-\bar{\Lambda} + \sigma_{+1}(\bar{\Lambda} - |\bar{\Lambda}|)]C\}_{i=n} \\ &\quad + \{C^T[+2\epsilon\bar{X} - 2\epsilon\sigma_{+1}\bar{X}]DC\}_{i=n} + \{\sigma_{+1}^3 C^1 C^3(\bar{\lambda}_1 - |\bar{\lambda}_1|)\}_{i=n} \\ &\quad + 2C_0^T g_{-1} - 2C_n^T g_{+1}. \end{aligned} \quad (42)$$

The choice $\sigma_{-1} = -I_3$ and $\sigma_{+1} = I_3$ leads to

$$\begin{aligned} \|C\|_I^2 &= -2\epsilon(\mathcal{D}C, \tilde{X}\mathcal{D}C)_H + 2(C, F)_P - [C^T \Lambda_I C - 2C^T g_{-1}]_{i=0} \\ &\quad - [C^T \Lambda_O C + 2C^T g_{+1}]_{i=n}, \end{aligned} \tag{43}$$

i.e., a growth rate which is exactly the same as in the continuous case (compare (43) with (16)). The definitions of Λ_I, Λ_O are given in (17). Integration of (43) leads to

$$\begin{aligned} \|C\|_P^2 + e^{\eta_D T} &\left\{ 2\epsilon \int_0^T (\mathcal{D}C, \tilde{X}\mathcal{D}C)_H e^{-\eta_D t} dt + \frac{\delta_D}{2} \int_0^T \|C\|_{\Gamma_D}^2 e^{-\eta_D t} dt \right\} \\ &\leq e^{\eta_D T} \left\{ \|f\|_P^2 + \frac{2}{\delta_D} \int_0^T \|g\|_{\Gamma_D}^2 e^{-\eta_D t} dt + \frac{1}{\eta_D} \int_0^T \|F\|_P^2 e^{-\eta_D t} dt \right\}. \end{aligned} \tag{44}$$

The estimate (44) is similar to (4) and hence (30) is a strongly stable approximation. The problem (30) is also strictly stable (we can choose $\eta_D = \eta$ and $\delta_D = \delta$; see (18), (5)). We can summarize the result in the following way.

THEOREM 3. *The approximation (30), (40), (41) of the problem (13), (14), (15) is both strictly and strongly stable if $\sigma_{-1} = -I_3$ and $\sigma_{+1} = I_3$.*

5.1.2. Accuracy

The problem describing the deviation $E_j = C(x_j, t) - C_j(t)$ between the exact continuous solution and the discrete approximation given by (30) is

$$\begin{aligned} E_t + \tilde{\Lambda}DE &= \epsilon \tilde{X}\mathcal{D}^2 E + P^{-1} [\sigma_{-1}(L_{-1}^D E) e_{-1} + \sigma_{+1}(L_{+1}^D E) e_{+1}] + T \\ E(0) &= 0. \end{aligned} \tag{45}$$

$T = T^{\text{DO}} + T^{\text{BC}}$ is the truncation error. T^{DO} and T^{BC} come from the approximation of the differential operator and the approximation of the boundary conditions, respectively. The truncation errors have the general structure

$$T^{\text{DO}} = \begin{pmatrix} \mathcal{O}(\Delta x^n) \\ \mathcal{O}(\Delta x^m) \\ \vdots \\ \mathcal{O}(\Delta x^m) \\ \mathcal{O}(\Delta x^n) \end{pmatrix}, \quad T^{\text{BC}} = \begin{pmatrix} \mathcal{O}(\Delta x^{(r-1)}) \\ 0 \\ \vdots \\ 0 \\ \mathcal{O}(\Delta x^{(r-1)}) \end{pmatrix}. \tag{46}$$

In [31, 32] it is shown that difference approximations to mixed hyperbolic-parabolic equations retain the accuracy of the interior scheme ($\mathcal{O}(\Delta x^m)$) if a finite number of points (independent of the total number) are closed with boundary stencils ($\mathcal{O}(\Delta x^n)$) that are one order less accurate. A requirement for that conclusion is that an energy estimate holds, which in turn means that the mathematical boundary conditions must be approximated to the order of the internal scheme. The discussion above implies that $n = m - 1$ and $r = m$ are necessary.

We will now apply the theory in [31, 32] to the type of difference approximations considered in this paper, i.e., where difference operators of the SBP type are used, together with a penalty formulation for the boundary conditions.

First, we split E and the T into two parts, i.e., $E = E^1 + E^2$ and $T = T^1 + T^2$, where

$$T^1 = \begin{pmatrix} 0 \\ g_1 \\ \vdots \\ g_{n-1} \\ 0 \end{pmatrix} = \mathcal{O}(\Delta x^m), \quad T^2 = \begin{pmatrix} g_0 \\ 0 \\ \vdots \\ 0 \\ g_n \end{pmatrix} = \mathcal{O}(\Delta x^{(m-1)}). \quad (47)$$

Next, we use the energy method to estimate E^1 . The energy method applied to (45) with E, T replaced by E^1, T^1 , and Theorem 3 leads directly to

$$\|E^1\|_P \leq \mathcal{O}(\Delta x^m).$$

Finally, we use the Laplace transform technique to take care of the boundary error and estimate E^2 . So far, the treatment has been general. However, in order to keep the algebraic complexity at a reasonable level, we now need to simplify and be specific. We will consider the inviscid ($\epsilon = 0$) Euler equations at an inflow boundary, where the first derivative is approximated with

$$D = \frac{1}{2\Delta x} \begin{pmatrix} -2 & 2 & & & & & \\ -1 & 0 & 1 & & & & \\ & \cdot & \cdot & \cdot & & & \\ & & \cdot & \cdot & \cdot & & \\ & & & -1 & 0 & 1 & \\ & & & & -2 & 2 & \end{pmatrix}, \quad P = \Delta x \begin{pmatrix} \frac{1}{2} & & & & & & \\ & 1 & & & & & \\ & & \cdot & & & & \\ & & & \cdot & & & \\ & & & & \cdot & & \\ & & & & & 1 & \\ & & & & & & \frac{1}{2} \end{pmatrix}. \quad (48)$$

The half-plane problem obtained by Laplace-transforming (45) with E, T replaced by E^2, T^2 becomes

$$\begin{aligned} \tilde{s} \hat{E}_0^2 + \bar{\lambda} (\hat{E}_1^2 - \hat{E}_0^2) &= \sigma_{-1} (\bar{\lambda} + |\bar{\lambda}|) \hat{E}_0^2 + \Delta x \hat{g}_0, \\ \tilde{s} \hat{E}_j^2 + \bar{\lambda} (\hat{E}_{j+1}^2 - \hat{E}_{j-1}^2)/2 &= 0, \quad j \geq 1, \\ \hat{E}_j^2 &\rightarrow 0, \quad j \rightarrow \infty, \end{aligned} \quad (49)$$

where $\tilde{s} = s \Delta x$. The second and third equations in (49) lead to

$$E_j^2 = \sigma_1 \begin{pmatrix} 1 \\ 0 \\ 0 \end{pmatrix} \kappa_1^j + \sigma_2 \begin{pmatrix} 0 \\ 1 \\ 0 \end{pmatrix} \kappa_2^j + \sigma_3 \begin{pmatrix} 0 \\ 0 \\ 1 \end{pmatrix} \kappa_3^j, \quad (50)$$

$$\kappa_j = \begin{cases} -(\tilde{s}/\lambda_j) + \sqrt{1 + (\tilde{s}/\lambda_j)^2}, & \lambda_j > 0, \\ 0, & \lambda_j = 0, \\ -(\tilde{s}/\lambda_j) - \sqrt{1 + (\tilde{s}/\lambda_j)^2}, & \lambda_j < 0, \end{cases} \quad (51)$$

where the branch of the square root is the one with positive real part for $\text{Re}(\tilde{s}) \geq 0$. The case when $\lambda_j = 0$ presents no problem; it only reduces the number of equations in (30). In the sequel, we assume $\lambda_j \neq 0$.

The first equation in (49) leads to

$$E(\tilde{s})\sigma = \Delta x \hat{g}_0, \quad E(\tilde{s}) = \text{diag}(\tilde{s} + \lambda_j \kappa_j - (\lambda_j + \sigma_{-1}^j(\lambda_j + |\lambda_j|))), \quad j = 1, 2, 3.$$

A nonsingular $E(\tilde{s})$, i.e.,

$$\det(E(\tilde{s})) \neq 0, \quad \text{Re}(\tilde{s}) \geq 0, \tag{52}$$

and (50), (51) lead to $|\hat{E}_j^2| \leq \text{const}|\Delta x \hat{g}_0|$ for $\text{Re}(\tilde{s}) \geq 0$; i.e., the Kreiss condition is satisfied. Parseval’s relation and the fact that $E_j^2(t)$ cannot depend on $g_0(T)$ for $t < T$ leads to

$$\int_0^t |E_j^2|^2 dt \leq \text{const} \int_0^t |\Delta x g_0|^2 dt, \quad j \geq 0.$$

Finally, since $g_0 = \mathcal{O}(\Delta x)$, we obtain

$$\|E^2\|_P \leq \mathcal{O}(\Delta x^2).$$

It still must be shown that (52) holds. The inviscid condition for strict stability $\lambda_j + \sigma_{-1}^j(\lambda_j + |\lambda_j|) \leq 0$ (see (42) and (51)), which implies $\tilde{s} + \lambda_j \kappa_j = |\lambda_j| \sqrt{1 + (\tilde{s}/\lambda_j)^2} \geq 0$, leads directly to (52). The procedure to estimate the boundary error at an outflow boundary is exactly the same as in the inflow case. We can summarize the result in the following theorem.

THEOREM 4. *The approximation (30), (40), (41) of the problem (13), (14), (15) is second-order accurate if Theorem 3 holds and the first derivative operator $\mathcal{D} = P^{-1}Q$ is given by (48).*

Remark. The procedure above (exemplified in the second-order accurate case) to prove accuracy is general. The last step where one uses the Laplace transform technique to estimate the boundary error E^2 is not necessary (i) if the boundary stencils have the same order of accuracy as the internal stencil, i.e., $n = m$, and (ii) if the approximation of the mathematical boundary conditions is one order more accurate, i.e., $r = m + 1$.

5.2. The Discrete Multiple Domain Problem

A finite difference approximation of the coupled problems (19) and (20) is

$$\begin{aligned} U_t + \tilde{\Lambda} \mathcal{D}_L U &= \epsilon \tilde{X} \mathcal{D}_L^2 U + F + B T_0 + P_L^{-1} (\sigma_L^I (U_n - V_0) \\ &\quad + \sigma_L^V ((\mathcal{D}_L U)_n - (\mathcal{D}_R V)_0)) e_L \\ U(0) &= f \\ V_t + \tilde{\Lambda} \mathcal{D}_R V &= \epsilon \tilde{X} \mathcal{D}_R^2 V + F + B T_m + P_R^{-1} (\sigma_R^I (V_0 - U_n) \\ &\quad + \sigma_R^V ((\mathcal{D}_R V)_0 - (\mathcal{D}_L U)_n)) e_R \\ V(0) &= f. \end{aligned} \tag{53}$$

The characteristic variables in the left (subscript L) $[x_0 = -1, x_n = 0]$ and right (subscript R) $[x_0 = 0, x_m = +1]$ domains are U and V , respectively, (see Fig. 1). $B T_0, B T_m$ denote the

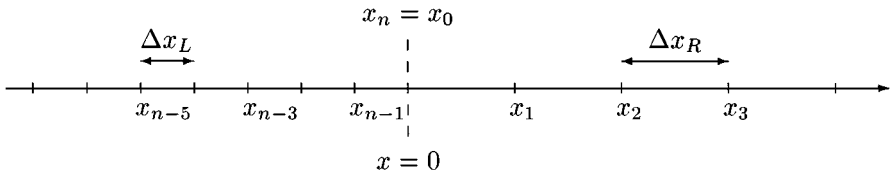


FIG. 1. The mesh close to the interface at $x = 0$.

boundary terms at $x = \pm 1$, respectively. Definitions of \mathcal{D} , \mathcal{D}^2 , $\tilde{\Lambda}$, \tilde{X} , e_{-1} , e_{+1} are given in (31), (32), (33), and $e_L = (0, \dots, 1)^T \otimes I_3$, $e_R = (1, \dots, 0)^T \otimes I_3$.

The values of σ_{-1} and σ_{+1} that lead to strict and strong stability for the discrete single domain problem are given in Theorem 3. We must still determine σ_L^I , σ_L^V , σ_R^I , σ_R^V . Note that the difference operators \mathcal{D}_L , \mathcal{D}_L^2 , \mathcal{D}_R , \mathcal{D}_R^2 can be different in the left and right domains and that $\Delta x_L \neq \Delta x_R$ in general.

5.2.1. Conservation

To calculate the strength and speed of a shock with finite mesh size, one needs a conservative scheme. Let us start by considering a continuous problem in conservation form, $u_t + f_x = 0$, $|x| \leq 1$, $t \geq 0$. Integration over the domain leads to

$$\frac{d}{dt} \int_{-1}^{+1} u \, dx + f_{+1} - f_{-1} = 0;$$

i.e., the total change of u in the domain is only due to the flux through the boundaries. Note that integration of f_x over the the domain reverses the differentiation process and leaves information only at the boundaries.

Let F , $\mathcal{D}F$ denote the numerical approximations of f , f_x . The discrete SBP derivative satisfies

$$f_x - \mathcal{D}f = T_{e1}, \quad \mathcal{D}f = P^{-1}Qf, \quad T_{e1} = \mathcal{O}(\Delta x^r). \quad (54)$$

Multiplying (54) with the operator $l^T P$, where $l^T = [1, 1, \dots, 1] \otimes I_p$ (f has p components) and observing that $f_{+1} - f_{-1} = \int_{-1}^{+1} f_x \, dx$ leads to

$$l^T P f_x = \int_{-1}^{+1} f_x \, dx + \mathcal{O}(\Delta x^r).$$

The operator $l^T P$ is the discrete integration operator. This operator reverses the process of differentiation, leaves information only at the boundaries, and converges to the continuous integration operator as $\Delta x \rightarrow 0$.

Remark. The linear continuous problem (13) considered in this paper does of course not produce any shocks. However, conservation is nevertheless a desirable property since we aim for a discrete approximation with the same behaviour as the linear continuous problem, which indeed is conservative. Moreover, it will be shown below (see the second Remark in Section 5.2.2) that the conditions for conservation are a subset of the necessary conditions for stability.

We will now prove the following theorem.

THEOREM 5. *The approximation (53) of the problem (13) is conservative if*

$$\sigma_L^I - \sigma_R^I - \bar{\Lambda} = 0, \quad \sigma_L^V - \sigma_R^V + \epsilon \bar{X} = 0, \tag{55}$$

where the matrices $\bar{\Lambda}$ and \bar{X} are given in (11).

Proof. Multiplying (53) with $l_L^T P_L$ and $l_R^T P_R$ leads to

$$\begin{aligned} (l_L^T P_L U + l_R^T P_R V)_t &= -(l_L^T Q_L \tilde{\Lambda} U + l_R^T \tilde{Q}_R \tilde{\Lambda} V) + \epsilon (l_L^T R_L \tilde{X} U + l_R^T R_R \tilde{X} V) \\ &\quad + (\sigma_L^I - \sigma_R^I)(U_N - V_0) + (\sigma_L^V - \sigma_R^V)(\mathcal{D}U_N - \mathcal{D}V_0) \\ &\quad + 2(U, F)_{P_L} + 2(V, F)_{P_R} + BT_{i=m}^{i=0}, \end{aligned} \tag{56}$$

where BT includes the boundary terms at $x = \pm 1$. To obtain (56) we have made use of Lemma 1.

The inviscid terms can be written

$$l_L^T Q_L \tilde{\Lambda} U + l_R^T Q_R \tilde{\Lambda} = -(\tilde{\Lambda} U)_0 + (\tilde{\Lambda} U)_n - (\tilde{\Lambda} V)_0 + (\tilde{\Lambda} V)_m. \tag{57}$$

Next, we consider the viscous terms. Both $R = QP^{-1}Q$ and $R = (-S^T M + D)S$ lead to

$$l_L^T Q_L P_L^{-1} Q_L \tilde{X} U + l_R^T Q_R P_R^{-1} Q_R \tilde{X} V = -(\tilde{X} \mathcal{D}U)_0 + (\tilde{X} \mathcal{D}U)_n - (\tilde{X} \mathcal{D}V)_0 + (\tilde{X} \mathcal{D}U)_m. \tag{58}$$

By inserting (57) and (58) into (56), neglecting the boundary terms at $x = \pm 1$, letting $F = 0$, and applying condition (55), we obtain $(l_L^T P_L U + l_R^T P_R V)_t = 0$; i.e., the approximation (53) is conservative. ■

5.2.2. Stability

We start with the following observation.

Remark. Stability of the one domain problem *does not* imply stability of the multiple domain problem. Stability means that the solution can be estimated in terms of the (bounded) boundary data. In a multiple domain problem, the boundary data are made up of the solution(s) in the other domain(s). Boundedness of the data would require an a priori assumption.

The main result of this paper is given below.

THEOREM 6. *The approximation (53) of the problem (13) is both strictly and strongly stable if*

$$\sigma_L^V = \sigma \epsilon \bar{X}, \quad \sigma_L^I = \frac{1}{2}(\bar{\Lambda} - \beta \epsilon \bar{X} - \delta I_3), \quad \beta \geq \frac{\sigma^2}{2\alpha_R} + \frac{(1 + \sigma)^2}{2\alpha_L}, \quad \delta \geq 0, \tag{59}$$

and if Theorems 3 and 5 hold. σ and δ are free parameters and α_L, α_R denote the minimal eigenvalue of P if $R = QP^{-1}Q$ and the minimal eigenvalue of $(M + M^T)/2$ if $R = (-S^T M + D)S$. The matrices $\bar{\Lambda}, \bar{X}$ are given in (11).

Proof. Strict and strong stability of (53) follows if the interface treatment at $x = 0$ is of a dissipative nature. For that reason we neglect the terms at the boundaries $x = \pm 1$ and use $F = 0$. The energy method leads to

$$\begin{aligned} \frac{d}{dt}(\|U\|_{P_L}^2 + \|V\|_{P_R}^2) &= -U^T(\tilde{\Lambda}Q_L + Q_L^T\tilde{\Lambda})U - V^T(\tilde{\Lambda}Q_R + Q_R^T\tilde{\Lambda})V \\ &\quad + \epsilon U^T(\tilde{X}R_L + R_L^T\tilde{X})U + \epsilon V^T(\tilde{X}R_R + R_R^T\tilde{X})V \\ &\quad + 2U_n^T(\sigma_L^I(U_n - V_0) + \sigma_L^V(DU_n - DV_0)) \\ &\quad + 2V_0^T(\sigma_R^I(V_0 - U_n) + \sigma_R^V(DV_0 - DU_n)). \end{aligned} \quad (60)$$

Equations (35), (36), and (37) lead to

$$-U^T(\tilde{\Lambda}Q_L + Q_L^T\tilde{\Lambda})U = U_0^T\tilde{\Lambda}U_0 - U_n^T\tilde{\Lambda}U_n \quad (61)$$

$$-V^T(\tilde{\Lambda}Q_R + Q_R^T\tilde{\Lambda})V = V_0^T\tilde{\Lambda}V_0 - V_m^T\tilde{\Lambda}V_m \quad (62)$$

$$U^T(\tilde{X}R_L + R_L^T\tilde{X})U \leq -2U_0\tilde{X}DU_0 + 2U_n\tilde{X}DU_n - 2\alpha_L DU_n^T\tilde{X}DU_n \quad (63)$$

$$V^T(\tilde{X}R_R + R_R^T\tilde{X})V \leq -2V_0\tilde{X}DV_0 + 2V_m\tilde{X}DV_m - 2\alpha_R DV_0^T\tilde{X}DV_0. \quad (64)$$

By inserting (61)–(64) into (60) and neglecting boundary terms at $x = \pm 1$ we obtain

$$\frac{d}{dt}(\|U\|_{P_L}^2 + \|V\|_{P_R}^2) \leq W^T E W,$$

where

$$W = \begin{pmatrix} U_n \\ V_0 \\ DU_n \\ DV_0 \end{pmatrix}, \quad E = \begin{pmatrix} 2\sigma_L^I - \bar{\Lambda} & -(\sigma_L^I + \sigma_R^I) & \sigma_L^V + \epsilon\tilde{X} & -\sigma_L^V \\ -(\sigma_L^I + \sigma_R^I) & 2\sigma_R^I + \bar{\Lambda} & -\sigma_R^V & \sigma_R^V - \epsilon\tilde{X} \\ \sigma_L^V + \epsilon\tilde{X} & -\sigma_R^V & -2\alpha_L\epsilon\tilde{X} & 0 \\ -\sigma_L^V & \sigma_R^V - \epsilon\tilde{X} & 0 & -2\alpha_R\epsilon\tilde{X} \end{pmatrix}.$$

The problem (53) is strictly and strongly stable if E is negative semidefinite. E is an almost full matrix; to obtain explicit stability conditions, simplifications of E are necessary. The energy method applied to the continuous multiple domain problem leads to (23) which suggests that the variables

$$\tilde{W} = \tilde{S}W = \frac{1}{\sqrt{2}} \begin{pmatrix} U_n - V_0 \\ U_n + V_0 \\ DU_n - DV_0 \\ DU_n + DV_0 \end{pmatrix}, \quad \tilde{S} = \frac{1}{\sqrt{2}} \begin{pmatrix} +I & -I & 0 & 0 \\ +I & +I & 0 & 0 \\ 0 & 0 & +I & -I \\ 0 & 0 & +I & +I \end{pmatrix}$$

are of interest. The use of these variables and the conservation conditions in Theorem 5 leads to

$$E_1 = \tilde{S}E\tilde{S}^T = \begin{pmatrix} 2(2\sigma_L^I - \bar{\Lambda}) & 0 & 2\sigma_L^V + \epsilon\tilde{X} & \epsilon\tilde{X} \\ 0 & 0 & 0 & 0 \\ 2\sigma_L^V + \epsilon\tilde{X} & 0 & -(\alpha_L + \alpha_R)\epsilon\tilde{X} & (\alpha_R - \alpha_L)\epsilon\tilde{X} \\ \epsilon\tilde{X} & 0 & (\alpha_R - \alpha_L)\epsilon\tilde{X} & -(\alpha_L + \alpha_R)\epsilon\tilde{X} \end{pmatrix}.$$

Remark. The first condition in Theorem 5 made the elements $(E_1)_{12} = (E_1)_{21}$ equal to zero. The second condition in Theorem 5 canceled the elements $(E_1)_{23} = (E_1)_{32}$. These conservation conditions are necessary in order to obtain negative semidefiniteness of E_1 since $(E_1)_{22}$ is zero.

To show that E_1 is negative semidefinite, introduce the first condition in (59). Second, add and subtract the matrix $-2\beta\epsilon\bar{X}$ to the upper left block in E_1 . The condition for negative semidefiniteness becomes

$$y_1^T (2(2\sigma_L^I - \bar{\Lambda}) + 2\beta\epsilon\bar{X})y_1 + \epsilon [(Y \otimes \bar{R})^T y_2]^T [\Lambda_{E_2} \otimes \bar{B}] [(Y \otimes \bar{R})^T y_2] \leq 0, \tag{65}$$

where $\bar{B} = \bar{R}^T \bar{X} \bar{R}$, $\Lambda_{E_2} = Y^T E_2 Y$, and

$$E_2 = \begin{pmatrix} -2\beta & (1 + 2\sigma) & 1 \\ (1 + 2\sigma) & -(\alpha_L + \alpha_R) & \alpha_R - \alpha_L \\ 1 & \alpha_R - \alpha_L & -(\alpha_L + \alpha_R) \end{pmatrix}.$$

The first term in (65) is nonpositive if the second relation in (59) holds. Negative definiteness that implies $\Lambda_{E_2} \leq 0$ is obtained if the third relation in (59) holds. ■

5.2.3. Accuracy

In this section we will consider the accuracy close to the interface. The procedure is similar to the one used in Section 5.1.2 for the single domain problem. The problem describing the deviations $\tilde{U}_j = U(x_j, t) - U_j(t)$ and $\tilde{V}_j = V(x_j, t) - V_j(t)$ between the exact continuous solutions and the discrete approximations given by (53) is

$$\begin{aligned} U_t + \tilde{\Lambda} \mathcal{D}_L U &= \epsilon \tilde{X} \mathcal{D}_L^2 U + T_L + P_L^{-1} [\sigma_L^I (U_n - V_0) + \sigma_L^V ((\mathcal{D}_L U)_n - (\mathcal{D}_R V)_0)] e_L \\ U(0) &= 0; \\ V_t + \tilde{\Lambda} \mathcal{D}_R V &= \epsilon \tilde{X} \mathcal{D}_R^2 V + T_R + P_R^{-1} [\sigma_R^I (V_0 - U_n) + \sigma_R^V ((\mathcal{D}_R V)_0 - (\mathcal{D}_L U)_n)] e_R \\ V(0) &= 0. \end{aligned} \tag{66}$$

For simplicity, we have used the notation $U = \tilde{U}$ and $V = \tilde{V}$. Note also that the terms at the boundaries $x = \pm 1$ are neglected. The treatment at the boundaries $x = \pm 1$ has been discussed in Section 5.1.2.

T_L and T_R are the truncation errors from the approximation of the differential operator and the interface conditions. The truncation errors have the general structure

$$T_L = \begin{pmatrix} \vdots \\ \mathcal{O}(\Delta x_L^m) \\ \mathcal{O}(\Delta x_L^{(m-1)}) \end{pmatrix}, \quad T_R = \begin{pmatrix} \mathcal{O}(\Delta x_R^{(n-1)}) \\ \mathcal{O}(\Delta x_R^n) \\ \vdots \end{pmatrix}.$$

The discussion in Section 5.1.2 on the size of the truncation error is applicable also for the interface problem.

Following the procedure in Section 5.1.2, one splits up the errors in two parts: the first part (T_L^1, T_R^1) contains the truncation error of the internal scheme; the second part contains a boundary contribution (T_L^2, T_R^2) with one order lower accuracy. The structure of these errors

are

$$T_L^1 = \begin{pmatrix} \vdots \\ \mathcal{O}(\Delta x_L^m) \\ 0 \end{pmatrix}, \quad T_L^2 = \begin{pmatrix} \vdots \\ 0 \\ \mathcal{O}(\Delta x_L^{(m-1)}) \end{pmatrix},$$

$$T_R^1 = \begin{pmatrix} 0 \\ \mathcal{O}(\Delta x_R^n) \\ \vdots \end{pmatrix}, \quad T_R^2 = \begin{pmatrix} \mathcal{O}(\Delta x_R^{(n-1)}) \\ 0 \\ \vdots \end{pmatrix}.$$

Also the error is divided into two parts; i.e., we consider $U = U^1 + U^2$ and $V = V^1 + V^2$.

By using the energy method, U^1 and V^1 will be bounded by T_L^1 and T_R^1 . This procedure is straightforward, entirely similar to the one in Section 5.1.2, and will therefore not be repeated here. Suffice it to say that the stability conditions given in Theorem 6 lead to

$$\|U^1\|_{P_L} + \|V^1\|_{P_R} \leq \mathcal{O}(\Delta x_L^n) + \mathcal{O}(\Delta x_R^m).$$

To bound U^2 and V^2 in terms of T_L^2 and T_R^2 requires use of the Laplace transform technique. That analysis is given in detail below.

Also in this case, we keep the algebraic complexity down by considering the inviscid ($\epsilon = 0$) Euler equations with the first derivative approximated with (48). The problem for $\hat{U}^2 = \hat{U}$ and $\hat{V}^2 = \hat{V}$ obtained by Laplace-transforming (66) becomes

$$\begin{aligned} \tilde{s}_L \hat{U}_n + \tilde{\Lambda}(\hat{U}_n - \hat{U}_{n-1}) &= 2\sigma_L^1(U_n - V_0) + \Delta x_L \hat{g}_L \\ \tilde{s}_R \hat{V}_0 + \tilde{\Lambda}(\hat{V}_1 - \hat{V}_0) &= 2\sigma_R^1(V_0 - U_n) + \Delta x_R \hat{g}_R \\ \tilde{s}_L \hat{U}_j + \tilde{\Lambda}(\hat{U}_{j+1} - \hat{U}_{j-1})/2 &= 0, \quad j \leq n-1, \\ \tilde{s}_R \hat{V}_j + \tilde{\Lambda}(\hat{V}_{j+1} - \hat{V}_{j-1})/2 &= 0, \quad j \geq 1, \\ \hat{U}_j &\rightarrow 0, \quad j \rightarrow -\infty, \\ \hat{V}_j &\rightarrow 0, \quad j \rightarrow \infty, \end{aligned} \tag{67}$$

where $\tilde{s}_L = s \Delta x_L$, $\tilde{s}_R = s \Delta x_R$, $\hat{g}_L = \mathcal{O}(\Delta x_L^{(n-1)})$, and $\hat{g}_R = \mathcal{O}(\Delta x_R^{(m-1)})$.

The last four equations in (67) lead to

$$U_j = \sigma_L^1 \begin{pmatrix} 1 \\ 0 \\ 0 \end{pmatrix} (\kappa_L^1)^{j-n} + \sigma_L^2 \begin{pmatrix} 0 \\ 1 \\ 0 \end{pmatrix} (\kappa_L^2)^{j-n} + \sigma_L^3 \begin{pmatrix} 0 \\ 0 \\ 1 \end{pmatrix} (\kappa_L^3)^{j-n}, \tag{68}$$

$$V_j = \sigma_R^1 \begin{pmatrix} 1 \\ 0 \\ 0 \end{pmatrix} (\kappa_R^1)^j + \sigma_R^2 \begin{pmatrix} 0 \\ 1 \\ 0 \end{pmatrix} (\kappa_R^2)^j + \sigma_R^3 \begin{pmatrix} 0 \\ 0 \\ 1 \end{pmatrix} (\kappa_R^3)^j, \tag{69}$$

$$\kappa_L^j = \begin{cases} -(\tilde{s}_L/\lambda_j) - \sqrt{1 + (\tilde{s}/\lambda_j)^2}, & \lambda_j > 0, \\ 0, & \lambda_j = 0, \\ -(\tilde{s}_L/\lambda_j) + \sqrt{1 + (\tilde{s}/\lambda_j)^2}, & \lambda_j < 0; \end{cases} \tag{70}$$

$$\kappa_R^j = \begin{cases} -(\tilde{s}_R/\lambda_j) + \sqrt{1 + (\tilde{s}/\lambda_j)^2}, & \lambda_j > 0, \\ 0, & \lambda_j = 0, \\ -(\tilde{s}_R/\lambda_j) - \sqrt{1 + (\tilde{s}/\lambda_j)^2}, & \lambda_j < 0, \end{cases} \tag{71}$$

where the branch of the square root is the one with a positive real part for $\text{Re}(\tilde{s}) \geq 0$. Also in this case, $\lambda_j = 0$ presents no problem, only the number of equations in (30) is reduced. We assume $\lambda_j \neq 0$ in the following.

The coefficients $\sigma_L = (\sigma_L^1, \sigma_L^2, \sigma_L^3)^T$ and $\sigma_R = (\sigma_R^1, \sigma_R^2, \sigma_R^3)^T$ will be determined by the first two equations in (67). They, together with the first condition in Theorem 5, lead to

$$E(\tilde{s}_L, \tilde{s}_R) \begin{pmatrix} \sigma_L \\ \sigma_R \end{pmatrix} = \begin{pmatrix} \Delta x_L \hat{g}_L \\ \Delta x_R \hat{g}_R \end{pmatrix}, \tag{72}$$

$$E(\tilde{s}_L, \tilde{s}_R) = \begin{pmatrix} \tilde{s}_L I_3 - \bar{\Lambda} \kappa_L^{-1} + \bar{\Lambda} - 2\sigma_L^I & 2\sigma_L^I \\ 2(\sigma_L^I - \bar{\Lambda}) & \tilde{s}_R I_3 + \bar{\Lambda} \kappa_R + \bar{\Lambda} - 2\sigma_R^I \end{pmatrix},$$

where $\kappa_L = \text{diag}(\kappa_L^1, \kappa_L^2, \kappa_L^3)$ and $\kappa_R = \text{diag}(\kappa_R^1, \kappa_R^2, \kappa_R^3)$.

A nonsingular $E(\tilde{s}_L, \tilde{s}_R)$ leads via the Kreiss condition and Parseval’s relation (see Section 5.1.2) to the estimate

$$\|U^2\|_{P_L} \leq \mathcal{O}(\Delta x_L^2) + \mathcal{O}(\Delta x_R^2), \quad \|V^2\|_{P_R} \leq \mathcal{O}(\Delta x_L^2) + \mathcal{O}(\Delta x_R^2).$$

It still must be shown that (52) for E , defined in (72), holds. A direct calculation using (72), (70), and (71) leads to

$$\text{Det}(E) = \prod_{j=1}^3 G_j,$$

$$G_j = |\lambda_j|^2 \left(1 + \sqrt{1 + (\tilde{s}_L/\lambda_j)^2} \sqrt{1 + (\tilde{s}_R/\lambda_j)^2} \right) + |\lambda_j| \sqrt{1 + (\tilde{s}_L/\lambda_j)^2} \sqrt{1 + (\tilde{s}_R/\lambda_j)^2}.$$

Let $\sqrt{1 + (\tilde{s}_L/\lambda_j)^2} = \eta_L + i\xi_L$ and $\sqrt{1 + (\tilde{s}_R/\lambda_j)^2} = \eta_R + i\xi_R$, where η_L, η_R are non-negative. A simple algebraic test reveals that the imaginary part and the real part of G_j cannot be zero at the same time if the inviscid condition for stability $\bar{\Lambda} - 2\sigma_L^I \leq 0$ in Theorem 6 holds. We can summarize the result in the following theorem.

THEOREM 7. *The approximation (53) of the problem (13) with $\epsilon = 0$ is second-order accurate; i.e.,*

$$\|U\|_{P_L} + \|V\|_{P_R} \leq \mathcal{O}(\Delta x_L^2) + \mathcal{O}(\Delta x_R^2),$$

if Theorem 6 holds and the first derivative operator $\mathcal{D} = P^{-1}Q$ is given by (48).

Remark. Also in the interface case (see Section 5.1.2) the procedure to prove accuracy, which was exemplified above in the second-order accurate case, is general. The last step in which one uses the Laplace transform technique to estimate the errors U^2 and V^2 is not necessary (i) if the stencils adjacent to the interface have the same order of accuracy as the internal stencil, and (ii) if the interface conditions are one order more accurate.

5.2.4. The Discrete Multiple Domain Problem in Conservation Form

The discrete multiple domain problem (53) can be transformed to conservative form by multiplying the equations with $I_{n+1} \otimes \bar{T}(\bar{R}\bar{S})^{-1}$, $I_{m+1} \otimes \bar{T}(\bar{R}\bar{S})^{-1}$, respectively. The result

is

$$\begin{aligned}
 U_t + P_L^{-1}(Q_L F^I - \epsilon R_L F^V) \\
 &= +(1/2)P_L^{-1}[(F_L^T - F_R^T) + (1 + 2\sigma)\epsilon(F_L^V - F_R^V) - F_L^B] \\
 V_t + P_R^{-1}(Q_R F^I - \epsilon R_R F^V) \\
 &= -(1/2)P_R^{-1}[(F_R^T - F_L^T) - (1 + 2\sigma)\epsilon(F_R^V - F_L^V) + F_R^B],
 \end{aligned} \tag{73}$$

where $F^T = F^I - \epsilon F^V$ and

$$F_L^B = (\delta I_3 + \epsilon \beta \bar{T} \bar{B} \bar{T}^{-1})(U_n - V_0), \quad F_R^B = (\delta I_3 + \epsilon \beta \bar{T} \bar{B} \bar{T}^{-1})(V_0 - U_n).$$

In (73), the forcing terms and the boundary conditions at $x \pm 1$ are neglected.

6. NUMERICAL EXPERIMENTS

By making one-dimensional computations using the nonlinear Euler and Navier–Stokes equations, we can check whether the theoretical conclusions drawn from the analysis of the constant coefficient problem agree with the results obtained in practice.

In the calculations below, we use the second-, fourth-, and sixth-order schemes reported in [24]. To integrate in time, a five-stage fourth-order RK scheme [33] has been used. Consider the stability condition (59). In the calculations below we have used $\sigma = -1/2$ and the conservative estimate $\sigma_L^I = \bar{\Lambda}/2 - \delta I$, where δ is determined through tests. Often we use $\delta = 1.0$. Equation (55) has been used to determine the other parameters.

First, we consider a sound propagation problem. The computational results, obtained using the nonlinear Euler equations at Mach number 0.5, are compared with an exact solution of the linearized problem. In Fig. 2, the errors for the second-, fourth-, and sixth-order schemes using one domain (1Dom), four uniform domains (4Dom), and eight randomly spaced domains (Rand) are shown. Clearly, the order of accuracy is independent of the presence and location of the interfaces. Due to the small amplitudes ($\propto 10^{-7}$) used in the sixth-order cases, we encounter roundoff, which can be seen as the kink on the sixth-order results.

Next, we consider a viscous shock propagation problem at Mach number 2.0 and Reynolds number 150. The exact solution of the Navier–Stokes equation for this case can be found in [34]. In Fig. 3, the errors for second-, fourth-, and sixth-order schemes using eight uniform domains (Unif) and eight randomly spaced domains (NonU) are shown. Also in this case, the order of accuracy is independent of the location of the interfaces.

The curves in the sixth-order case are not straight (see Fig. 3). The reason for this is that the curves are formed as a mean value of 15 simulations, where different wave speeds (w_s) ranging from -0.25 to 0.5 are used. The individual results for each wave speed vary slightly and lead to the nonstraight lines. Note that the trends are identical between the nonuniform and uniform cases.

In Fig. 4, the propagating shock ($w_s = 0.25$) for four different times is shown. In this case, the sixth-order scheme and 24 gridpoints were used in each domain.

Finally, we will discuss two additional questions concerning accuracy and stability/efficiency. The influence of interface conditions on accuracy is illustrated in Table I. The calculations are run to a physical time $T = 3$ at Mach number 2.0 and Reynolds number

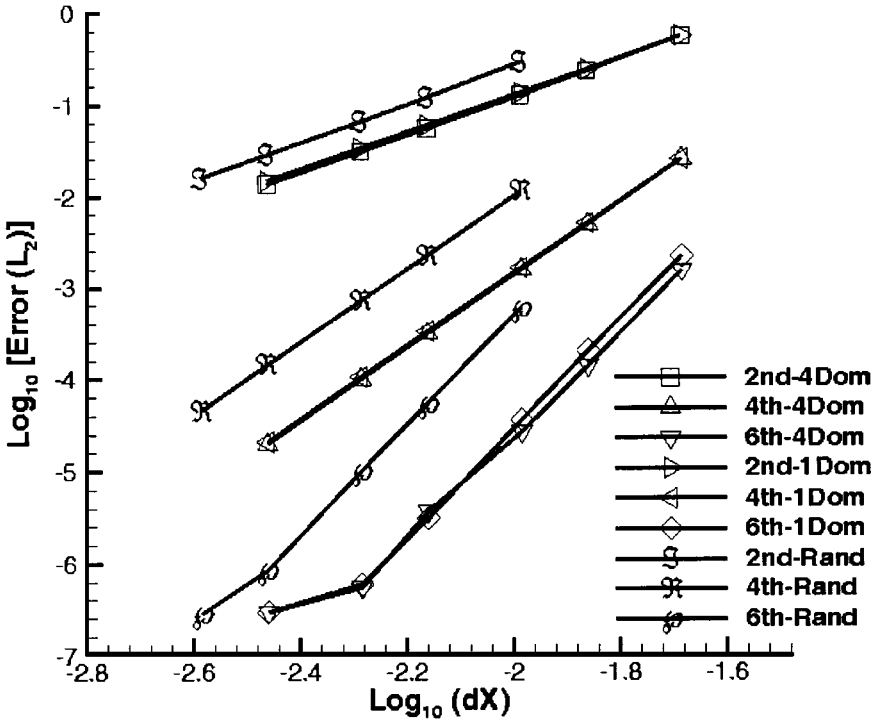


FIG. 2. Euler sound propagation. L_2 errors in calculations using the Euler equations.

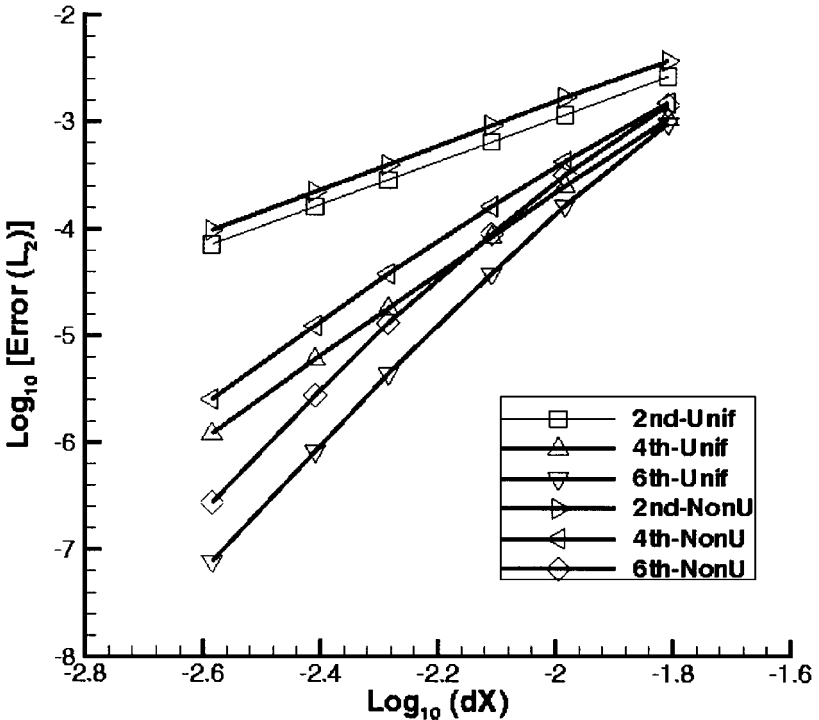


FIG. 3. Viscous shock propagation. L_2 errors in calculations using the Navier–Stokes equations.

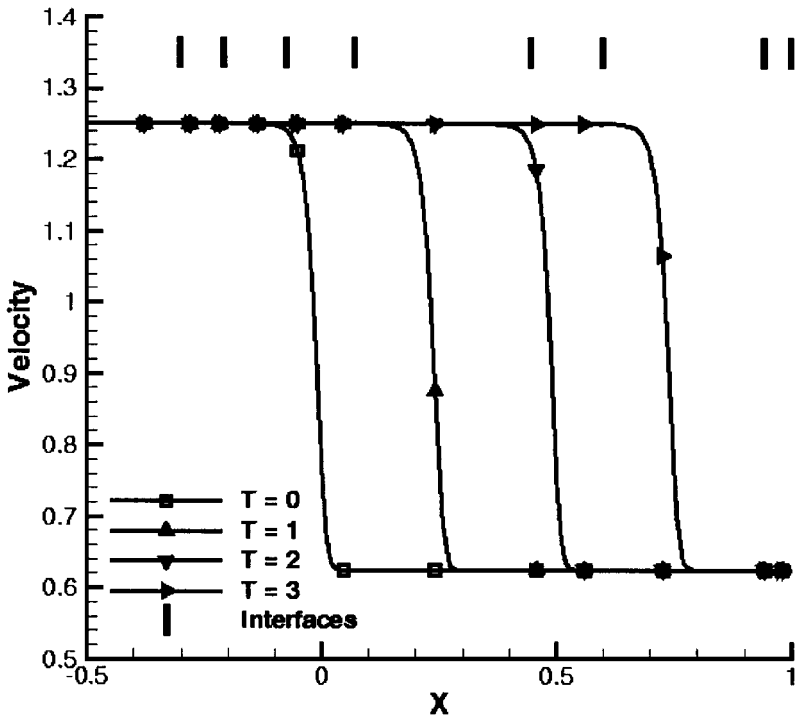


FIG. 4. Viscous shock propagation. A domain with randomly spaced interfaces.

$Re = 250$. The sixth-order SBP scheme is used, and the number of total points is 289 evenly distributed on the interval $-1/2 \leq x \leq 1$. The parameter in the study is the number of subdomains, keeping the total number of points constant. The number of subdomains ranges from 1 to 24. With 24 subdomains, the spatial operator involves 12 boundary stencils (fifth-order) and one sixth-order interior stencil. No further divisions are possible when using the sixth-order SBP operator. Note that this case is only marginally less accurate than the single domain case, for which the most points are discretized with sixth-order stencils.

The previous study indicates that there is little loss of accuracy when subdividing the domain. There are, however, other costs associated with domain subdivision. Introduction

TABLE I
Variation of L_2 Error on the
Number of Subdomains with
Grid Density Constant

Subdomains	LOG_{10} error
1	-4.527
2	-4.584
4	-4.457
8	-4.643
12	-4.313
16	-4.467
18	-4.342
24	-4.358

TABLE II
Variation of CFL Number and L_2 Error with Reynolds Number
for Single and Multiple Domain Cases

Re	LOG ₁₀ error	CFL _{max}	LOG ₁₀ error	CFL _{max}
1000	-2.154	0.55	DNC	
900	-2.242	0.55	-2.265	0.30
800	-2.347	0.55	-2.376	0.30
700	-2.477	0.60	-2.517	0.30
600	-2.637	0.60	-2.698	0.30
500	-2.841	0.60	-2.935	0.30
300	-3.429	0.65	-3.617	0.30
200	-4.027	0.65	-4.185	0.35
100	-5.741	0.60	-5.699	0.35
40	-7.892	0.50	-7.331	0.20
20	-9.535	0.45	-8.637	0.20
10	-10.968	0.40	-10.665	0.18

Note. DNC is short for “did not converge.”

of additional interfaces into the domain changes the resulting eigenspectrum of the semi-discrete operator. In [22], a reduction in the effective CFL, when using a penalty boundary procedure, was observed. We experience a similar reduction in the stability envelop as the number of subdomains is increased.

In Table II, a study compares the effective CFL of a single domain calculation, with those from a comparable grid divided into eight subdomains. Plotted are the errors and the maximum stable CFL as a function of the Reynolds numbers for the two cases. Note that while the errors are nearly equivalent for the two test cases, the maximum CFL for the single domain case is nearly a factor of 2 larger.

In practice, using more than eight subdomains does not further reduce the effective CFL. Specifically, a gradual decrease in CFL is observed until an asymptotic value is achieved at approximately eight subdomains. The two test cases used in this study (one and eight domains) represent the limits of stability experienced in practice. Work continues to eliminate this reduction in CFL, although acceptable efficiency is achieved with the method in its current form.

7. SUMMARY AND CONCLUSIONS

We have analyzed boundary conditions and interface conditions for the one-dimensional Euler and Navier–Stokes equations. Both the continuous and semidiscrete problems have been considered.

We have considered summation-by-parts operators and derived strictly and strongly stable boundary and interface conditions for the Euler and Navier–Stokes equations. We have also considered the question of accuracy, both in the general case and more specifically for a second-order accurate approximation of the Euler equations.

The interface conditions are stable and conservative even if the finite difference operators and mesh sizes vary from domain to domain. Numerical experiments which include a sound propagating problem and a viscous shock propagating problem show that the new conditions lead to accurate and stable results for the corresponding nonlinear problems also.

It was also shown by numerical experiments that there is little loss of accuracy associated with domain subdivision. However, the introduction of interfaces into the domain changed the eigenspectrum of the semidiscrete operator and caused a reduction of the CFL number by approximately a factor of 2.

REFERENCES

1. C. Tam and J. Webb, Dispersion-relation-preserving finite difference schemes for computational acoustics, *J. Comput. Phys.* **107**(2), (1993).
2. C. Tam, Computational aeroacoustics: Issues and methods, *AIAA J.* **33**(10), (1995).
3. C. Pruett, T. Zang, C. Chang, and M. Carpenter, Spatial direct numerical simulation of high speed boundary-layer flows. Part I. Algorithmic considerations and validation, *Theor. Comput. Fluid Dyn.* **7** (1995).
4. H. Jurgens and D. Zing, Implementation of a high-accuracy finite-difference scheme for linear wave phenomena, in *Proceedings from ICOSAHOM 95, 1995*, Paper 16.
5. A. Taflove, Re-inventing electromagnetic supercomputing solution of Maxwell's equations via direct time integration on space grid, in *30th AIAA Aerospace Sciences Meeting, Reno, Nevada, 1992*, Paper 92-0333.
6. W. Don and C. Quille, Resolution study for the numerical simulation of reactive flows, in *Proceedings from ICOSAHOM 95, 1995*, Paper 24.
7. H. O. Kreiss and J. Olinger, Comparison of accurate methods for the integration of hyperbolic equations, *Tellus* **24**(3), (1972).
8. P. Olsson, High-order difference methods and data-parallel implementation, Ph.D. thesis, Department of Scientific Computing, Uppsala University, 1992.
9. B. Strand, High-order difference approximations for hyperbolic initial boundary value problems, Ph.D. thesis, Department of Scientific Computing, Uppsala University, 1996.
10. G. Scherer, On energy estimates for difference approximations to hyperbolic partial differential equations, Ph.D. thesis, Department of Scientific Computing, Uppsala University, 1977.
11. H. O. Kreiss and G. Scherer, Finite element and finite difference methods for hyperbolic partial differential equations, in *Mathematical Aspects of Finite Elements in Partial Differential Equations* (Academic Press, New York, 1974).
12. M. H. Carpenter, D. Gottlieb, and S. Abarbanel, The stability of numerical boundary treatments for compact high-order finite-difference schemes, *J. Comput. Phys.* **108**(2), (1994).
13. B. Gustafsson, H. O. Kreiss, and Sunström, Stability theory of difference approximations for mixed initial boundary value problems, *Math. Comp.* **26**(119), (1972).
14. P. Olsson, Summation by parts, projections, and stability I, *Math. Comp.* **64**, 1035 (1995).
15. P. Olsson, Summation by parts, projections, and stability II, *Math. Comp.* **64**, 1473 (1995).
16. M. H. Carpenter, D. Gottlieb, and S. Abarbanel, Time-stable boundary conditions for finite-difference schemes solving hyperbolic systems: Methodology and application to high-order compact schemes, *J. Comput. Phys.* **111**(2), (1994).
17. B. Gustafsson, H. O. Kreiss, and J. Olinger, Time dependent problems and difference methods (Wiley, New York, 1996).
18. B. Gustafsson and P. Olsson, Fourth-order difference methods for hyperbolic IBVPs, *J. Comput. Phys.* **117** (1995).
19. B. Sjögren, High-order centered difference methods for the compressible Navier–Stokes equations, *J. Comput. Phys.* **117** (1995).
20. J. Hyman, M. Shashkov, J. Castillo, and S. Steinberg, High order mimetic finite difference methods on nonuniform grids, in *Proceedings from ICOSAHOM 95, 1995*, Paper 11.
21. D. A. Kopriva, Spectral methods for the Euler equations, the blunt body problem revisited, *AIAA J.* **29**, 1458 (1991).
22. J. S. Hesthaven and D. Gottlieb, A stable penalty method for the compressible Navier–Stokes equations. 1. Open boundary conditions, *SIAM J. Sci. Comput.* **17**(3), 579 (1996).

23. J. S. Hesthaven, A stable penalty method for the compressible Navier–Stokes equations. II. One-dimensional domain decomposition schemes, *SIAM J. Sci. Comput.* **18**(3), (1997).
24. M. H. Carpenter, J. Nordström, and D. Gottlieb, *A Stable and Conservative Interface Treatment of Arbitrary Spatial Accuracy*, NASA/CR-1998-206921, ICASE Report No. 98-12, Langley Research Center, Hampton, VA, 1998.
25. C. Van Loan, *Computational Frameworks for the Fast Fourier Transform* (SIAM, Philadelphia, 1992).
26. H. O. Kreiss and J. Lorenz, *Initial Boundary Value Problems and the Navier–Stokes Equations* (Academic Press, San Diego, 1989).
27. J. Nordström, The use of characteristic boundary conditions for the Navier–Stokes equations, *Comput. & Fluids* **24**(5), 609 (1995).
28. J. Nordström, The influence of open boundary conditions on the convergence to steady state for the Navier–Stokes equations, *J. Comput. Phys.* **85**, 210 (1989).
29. B. Strand, Summation by parts for finite difference approximations for d/dx , *J. Comput. Phys.* **110**(1), 47 (1994).
30. M. H. Carpenter and J. Otto, High-order cyclo-difference techniques: An alternative to finite differences, *J. Comput. Phys.* **118**, 242 (1995).
31. B. Gustafsson, The convergence rate for difference approximations to mixed initial boundary value problems, *Math. Comp.* **29**, 396 (1975).
32. B. Gustafsson, The convergence rate for difference approximations to general mixed initial boundary value problems, *SIAM J. Numer. Anal.* **18**(2), (1981).
33. M. H. Carpenter and C. A. Kennedy, *Fourth-Order 2N-Storage Runge–Kutta Schemes*, NASA-TM-109111, April 1994.
34. F. M. White, *Viscous Fluid Flow* (McGraw–Hill, New York, 1974).